

## Chapter 6

# Towards Computational Rules: Feynman Diagrams

As the basic tool to describe the physics of elementary particles, the final aim of quantum field theory is the calculation of observables. Most of the information we have about the physics of subatomic particles comes from scattering experiments. Typically, these experiments consist of arranging two or more particles to collide with a certain energy and to setup an array of detectors, sufficiently far away from the region where the collision takes place, that register the outgoing products of the collision and their momenta (together with other relevant quantum numbers).

Next we discuss how these cross sections can be computed from quantum mechanical amplitudes and how these amplitudes themselves can be evaluated in perturbative quantum field theory. We keep our discussion rather heuristic and avoid technical details that can be found in standard texts (see Ref. [1–15] of [Chap. 1](#)). The techniques described will be illustrated with the calculation of the cross section for Compton scattering at low energies and its application to the study of the polarization of the cosmic microwave background radiation. Exceptionally, and in order to better show the computational power of the diagrammatic tools in quantum field theory, these calculations will be presented in some detail.

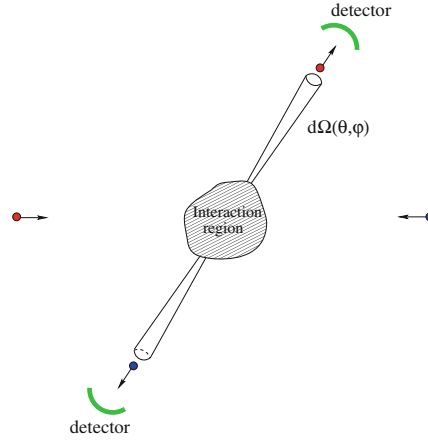
### 6.1 Cross Sections and S-Matrix Amplitudes

In order to fix ideas, we consider the simplest case of a collision experiment where two particles collide to produce again two particles in the final state. The aim of such an experiment is a direct measurement of the number of particles per unit time  $\frac{dN}{dt}(\theta, \varphi)$  registered by the detector within a solid angle  $d\Omega$  in the direction specified by the polar angles  $\theta, \varphi$  (see [Fig. 6.1](#)). On general grounds, we know that this quantity has to be proportional to the flux of incoming particles<sup>1</sup>  $f_{\text{in}}$ . The proportionality constant defines the differential cross section

---

<sup>1</sup> This is defined as the number of particles that enter the interaction region per unit time and per unit area perpendicular to the direction of the beam.

**Fig. 6.1** Schematic setup of a two-to-two-particles scattering event in the center of mass reference frame



$$\frac{dN}{dt}(\theta, \varphi) = f_{\text{in}} \frac{d\sigma}{d\Omega}(\theta, \varphi). \quad (6.1)$$

In natural units  $f_{\text{in}}$  has dimensions of  $(\text{length})^{-3}$ , so the differential cross section has dimensions of  $(\text{length})^2$ . It depends, apart from the direction  $(\theta, \varphi)$ , on the parameters of the collision (energy, impact parameter, etc.) as well as on the masses and spins of the incoming and outgoing particles.

The differential cross section measures the angular distribution of the products of the collision. It is also physically interesting to quantify how effective the interaction between the particles is in order to produce a nontrivial dispersion. This is measured by the total cross section, which is obtained by integrating the differential cross section over all directions

$$\sigma = \int_{-1}^1 d(\cos\theta) \int_0^{2\pi} d\varphi \frac{d\sigma}{d\Omega}(\theta, \varphi). \quad (6.2)$$

To gain some physical intuition on the meaning of the total cross section, we can think of the classical scattering of a point particle off a sphere of radius  $R$ . The particle undergoes a collision only when the impact parameter is smaller than the radius of the sphere and a calculation of the total cross section yields  $\sigma = \pi R^2$ . This is precisely the cross area that the sphere presents to incoming particles.

The starting point for the calculation of cross sections is the probability amplitude for the corresponding process. In a scattering experiment, one prepares a system with a given number of particles with definite momenta  $\mathbf{p}_1, \dots, \mathbf{p}_n$ . In the Heisenberg picture this is described by a time independent state labelled by the incoming momenta of the particles (to keep things simple we consider spinless particles) that we denote by

$$|p_1, \dots, p_n; \text{in}\rangle. \quad (6.3)$$

As a result of the scattering, a number  $k$  of particles with momenta  $\mathbf{p}'_1, \dots, \mathbf{p}'_k$  are detected. Thus, the system is now in the “out” Heisenberg picture state

$$|p'_1, \dots, p'_k; \text{out}\rangle \quad (6.4)$$

labelled by the momenta of the particles detected at late times. The probability amplitude of detecting  $k$  particles in the final state with momenta  $\mathbf{p}'_1, \dots, \mathbf{p}'_k$  in the collision of  $n$  particles with initial momenta  $\mathbf{p}_1, \dots, \mathbf{p}_n$  defines the  $S$ -matrix amplitude

$$S(\text{in} \rightarrow \text{out}) = \langle p'_1, \dots, p'_k; \text{out} | p_1, \dots, p_n; \text{in} \rangle. \quad (6.5)$$

It is very important to keep in mind that both (6.3) and (6.4) are time-independent states in the Hilbert space of a very complicated interacting theory. However, since both at early and late times the incoming and outgoing particles are far apart from each other, the “in” and “out” states can be thought as two states  $|p_1, \dots, p_n\rangle$  and  $|p'_1, \dots, p'_k\rangle$  in the Fock space of the corresponding free theory. Then, the overlaps (6.5) can be written in terms of the matrix elements of an  $S$ -matrix operator  $\hat{S}$  acting on the free Fock space

$$\langle p'_1, \dots, p'_k; \text{out} | p_1, \dots, p_n; \text{in} \rangle = \langle p'_1, \dots, p'_k | \hat{S} | p_1, \dots, p_n \rangle. \quad (6.6)$$

The operator  $\hat{S}$  is unitary,  $\hat{S}^\dagger = \hat{S}^{-1}$ , Lorentz invariant and its matrix elements are analytic in the external momenta.

In a scattering experiment there is the possibility that the particles do not interact at all and the system is left in the same initial state. It is useful to factor out this possibility from the  $S$ -matrix elements between initial and final states by writing

$$\hat{S} = \mathbf{1} + i\hat{T}, \quad (6.7)$$

where  $\mathbf{1}$  represents the identity operator. In this way, all nontrivial interactions are encoded in the matrix elements of the  $T$ -operator,  $\langle p'_i, \dots, p'_k | i\hat{T} | p_1, \dots, p_n \rangle$ . Furthermore, in these matrix elements it is convenient to factor out a delta function implementing momentum conservation to define the invariant scattering amplitude,  $i\mathcal{M}_{i \rightarrow f}$

$$\langle f | \hat{S} | i \rangle = \langle f | i \rangle + (2\pi)^4 \delta^{(4)} \left( \sum_{\text{final}} p'_i - \sum_{\text{initial}} p_j \right) i\mathcal{M}_{i \rightarrow f}. \quad (6.8)$$

Using the Lorentz invariance of the  $S$ -matrix it is not difficult to show that  $i\mathcal{M}_{i \rightarrow f}$  is a relativistic invariant as well (hence its name). Our next task is to show how observable quantities such as decay rates or cross sections can be obtained from the knowledge of this invariant amplitude. Then we will turn to the problem of computing the amplitude itself in quantum field theory.

In studying a scattering problem in the infinite volume limit we would have to consider localized wave packets for the asymptotic in and out states. Although this

can be done, it is rather cumbersome. This is the reason why we are going to employ a common trick consisting in working with plane waves for the in and out states, while putting the system at the same time in a space-time box of finite but large volume  $VT$ . We will see how at the end of the calculation all dependence on the size of the box drops out and the limit  $V \rightarrow \infty, T \rightarrow \infty$  can be taken safely.

The probability amplitude for the process is  $|\langle f | \hat{S} | i \rangle|^2$  which, for nontrivial transitions, is given by the modulus squared of the second term on the right-hand side of Eq. (6.8). The presence of the momentum conservation delta function makes the computation problematic. This is precisely where working at finite volume comes handy. The idea is to write one of the delta functions in terms of its Fourier transform

$$\begin{aligned} \left| (2\pi)^4 \delta^{(4)} \left( \sum_{\text{final}} p'_i - \sum_{\text{initial}} p_j \right) \right|^2 &= (2\pi)^4 \delta^{(4)} \left( \sum_{\text{final}} p'_i - \sum_{\text{initial}} p_j \right) \\ &\quad \times \int d^4x \exp \left[ i \left( \sum_{\text{final}} p'_i - \sum_{\text{initial}} p_j \right) \cdot x \right]. \end{aligned} \quad (6.9)$$

The remaining delta function then sets the argument of the exponential to zero and we have

$$\left| (2\pi)^4 \delta^{(4)} \left( \sum_{\text{final}} p'_i - \sum_{\text{initial}} p_j \right) \right|^2 = VT (2\pi)^4 \delta^{(4)} \left( \sum_{\text{final}} p'_i - \sum_{\text{initial}} p_j \right). \quad (6.10)$$

With this result we can compute the non-diagonal probability amplitude  $|\langle f | \hat{S} | i \rangle|^2$ . Dividing by  $T$ , the transition probability per unit time is given by

$$w_{i \rightarrow f} = V (2\pi)^4 \delta^{(4)} \left( \sum_{\text{final}} p'_i - \sum_{\text{initial}} p_j \right) |i \mathcal{M}_{i \rightarrow f}|^2. \quad (6.11)$$

In both scattering and decay processes, the final states have a continuous energy spectrum. To compute the probability for the particles in the final state to have momenta in a volume element  $d^3 p'_1 \cdots d^3 p'_k$  around  $(\mathbf{p}'_1, \dots, \mathbf{p}'_k)$ , we should multiply (6.11) by the number of states contained in it. Let us assume we have one particle in the volume  $V$  (or in other words, that the state is normalized to one). The number of available states within a momentum space volume element  $d^3 p$  can be directly written as

$$\frac{V d^3 p}{(2\pi \hbar)^3}, \quad (6.12)$$

where we have momentarily restored the powers of  $\hbar$  so the reader can clearly identify the density of states in phase space.

In the calculation of the  $S$ -matrix elements at infinite volume, the one-particle states  $|p\rangle$  satisfy the relativistic normalization (2.20). By putting the system in a

box of large volume  $V$ , the states become normalizable with  $\langle p|p\rangle = 2E_{\mathbf{p}}V$ . Thus, if we insist in using (6.12) for the final density of states of each outgoing particle we should not compute the  $S$ -matrix element between the relativistically normalized states  $|p\rangle$  but rather between the properly normalized ones  $(2E_{\mathbf{p}}V)^{-1/2}|p\rangle$ . Thus, since the probability amplitude involves the modulus *squared* of the amplitude, to find the correct expression for the number of states we should correct Eq. (6.12) by the normalization factor of the final states

$$\frac{Vd^3p}{(2\pi\hbar)^3} \frac{1}{2E_{\mathbf{p}}V} = \frac{d^3p}{(2\pi\hbar)^3} \frac{1}{2E_{\mathbf{p}}}. \quad (6.13)$$

We see how the volume cancels out and the infinite volume limit can be taken safely. Moreover, the resulting expression is relativistically invariant. Doing this for every particle in the final state of the scattering/decay process leads to the so-called *phase space factor*

$$d\Phi_k = \prod_{i=1}^k \frac{d^3p'_i}{(2\pi)^3} \frac{1}{2E'_i}, \quad (6.14)$$

where  $E'_i = \sqrt{m_i^2 + \mathbf{p}'_i{}^2}$  and we have restored natural units.

After this preliminary discussion we can compute the particle decay rate where we have a single particle in the initial state with momentum  $\mathbf{p}$ . As explained above, the proper normalization of the initial state introduces an extra factor of  $(2E_{\mathbf{p}}V)^{-1}$  in the square of the  $S$ -matrix element leading to (6.11). This has the effect of removing the remaining volume dependence, and we obtain the decay width

$$d\Gamma = \frac{1}{2E_{\mathbf{p}}} (2\pi)^4 \delta^{(4)}\left(p - \sum_{j=1}^k p'_j\right) |\mathcal{M}_{i\rightarrow f}|^2 d\Phi_k. \quad (6.15)$$

To calculate the total rate for this particular decay channel we should integrate over all final momenta. In doing that it is important to bear in mind that one has to divide the expression by a factor  $\prod_a n_a!$ , where  $n_a$  is the number of identical particles of type  $a$ . This is crucial to avoid overcounting the number of final states.

Here we notice that the factor of  $E_{\mathbf{p}}^{-1}$  in front of (6.15) has a simple physical meaning. Its suppression effect for large  $|\mathbf{p}|$  accounts for the relativistic effect of time dilation due to the motion of the decaying particle. In the rest frame this is equal to the rest mass  $m$ . The calculation of the total decay width for a particle requires not only to integrate over final momenta but also to sum over all possible decay channels, namely

$$\Gamma_{\text{total}} = \sum_{\text{channels}} \Gamma_i, \quad (6.16)$$

where  $\Gamma_i$  is the width of the  $i$ th decay channel. The lifetime of the particle is given by the inverse of the total width  $\Gamma_{\text{total}}$ .

We study now the calculation of the differential and total cross sections in the scattering of two particles with an arbitrary number of particles in the final state. The differential cross section for this problem is given by the number of particles scattered within an infinitesimal solid angle along the final momenta  $\mathbf{p}'_1, \dots, \mathbf{p}'_k$  divided by the flux of incoming particles  $f_{\text{in}}$ , thus generalizing Eq. (6.1). In terms of the probability density per unit time computed in Eq. (6.11), this gives

$$d\sigma = \frac{1}{4E_1 E_2 V^2} \frac{w_{i \rightarrow f}}{f_{\text{in}}} d\Phi_k \quad (6.17)$$

To get this expression we have multiplied by  $(2E_1 V)^{-1} (2E_2 V)^{-1}$  to take care of the normalization of the incoming states as discussed previously.

We need to compute the incoming flux  $f_{\text{in}}$ . The number of particles approaching the target (say particle 2) in a time  $dt$  across a surface  $dS$  orthogonal to the beam is given by  $n|\mathbf{v}_1 - \mathbf{v}_2| dt dS$ , with  $n$  the number density of projectiles (in this case the particle 1). Since in the calculation of the  $S$ -matrix amplitude we have normalized our states such that there is one particle per unit volume, we have that  $n = V^{-1}$  and the incoming flux is  $f_{\text{in}} = |\mathbf{v}_1 - \mathbf{v}_2|/V$ . Plugging this result into (6.17), we see how the powers of the volume cancel out and the differential cross section in the infinite volume limit reads

$$d\sigma = \frac{|\mathcal{M}_{i \rightarrow f}|^2}{4E_1 E_2 |\mathbf{v}_1 - \mathbf{v}_2|} (2\pi)^4 \delta^{(4)} \left( p_1 + p_2 - \sum_{j=1}^n p'_j \right) d\Phi_k, \quad (6.18)$$

where  $d\Phi_k$  is the phase space factor for the  $k$  particles in the final state. To calculate the total cross section we have to integrate over all final momenta and include the necessary symmetry factors if identical particles are produced as the result of the collision.

An inspection of Eq. (6.18) shows that the only piece depending on the observer's frame is the denominator  $F \equiv 4E_1 E_2 |\mathbf{v}_1 - \mathbf{v}_2|$ . The presence of this term implies that the measurement of the differential and total cross sections of the same collision in various reference frames takes different values. This is an important point that we discuss now in some detail.

We consider first a collinear reference frame in which the momenta of the two colliding particles lie along the same direction,  $\mathbf{p}_1 \parallel \mathbf{p}_2$ . This class of frames include two cases of particular interest: the laboratory frame, where one of the particles is at rest (for example  $\mathbf{p}_2 = 0$ ), and the center of mass frame where the center of mass is at rest,  $\mathbf{p}_2 = -\mathbf{p}_1$ .

It is not difficult to check that in the collinear case the combination  $E_1 E_2 |\mathbf{v}_1 - \mathbf{v}_2|$  is invariant under boosts along the direction of the two incoming momenta. This means that the value of the differential and total cross section is the same in *all* collinear frames. Moreover, we can write

$$\begin{aligned} F_{\text{coll}} &= 4E_1 E_2 |\mathbf{v}_1 - \mathbf{v}_2| = 4E_1 E_2 \left| \frac{\mathbf{p}_1}{E_1} - \frac{\mathbf{p}_2}{E_2} \right| \\ &= 4|E_2 \mathbf{p}_1 - E_1 \mathbf{p}_2| = 4(E_2 |\mathbf{p}_1| + E_1 |\mathbf{p}_2|), \end{aligned} \quad (6.19)$$

where in writing the last identity we have used that in the collinear frames the two particles are approaching each other from opposite directions. It can be written in a Lorentz invariant form

$$F_{\text{coll}} = 4\sqrt{(p_1 \cdot p_2)^2 - m_1^2 m_2^2}. \quad (6.20)$$

Then, the differential cross section measured in a collinear frame is given by

$$d\sigma_{\text{coll}} = \frac{|\mathcal{M}_{i \rightarrow f}|^2}{4\sqrt{(p_1 \cdot p_2)^2 - m_1^2 m_2^2}} (2\pi)^4 \delta^{(4)} \left( p_1 + p_2 - \sum_{j=1}^n p'_j \right) d\Phi_k. \quad (6.21)$$

The corresponding total cross section is obtained by integrating over all momenta in the final state, namely

$$\begin{aligned} \sigma_{\text{coll}} &= \frac{1}{4\sqrt{(p_1 \cdot p_2)^2 - m_1^2 m_2^2}} \int \left[ \prod_{\text{final states}} \frac{d^3 p'_i}{(2\pi)^3} \frac{1}{2E'_i} \right] \\ &\times |\mathcal{M}_{i \rightarrow f}|^2 (2\pi)^4 \delta^{(4)} \left( p_1 + p_2 - \sum_{\text{final states}} p'_i \right). \end{aligned} \quad (6.22)$$

We will make use of this expression in [Sect. 6.4](#) when studying Compton scattering.

Due to their invariance under Lorentz transformations, Eqs. (6.21) and (6.22) allow the computation in an arbitrary frame of the cross section measured by the collinear observer. For example, in a general frame where the two particles collide with velocities  $\mathbf{v}_1$  and  $\mathbf{v}_2$  the collinear cross section is obtained by using the following expression for  $F_{\text{coll}}$

$$F_{\text{coll}} = 4E_1 E_2 \sqrt{(\mathbf{v}_1 - \mathbf{v}_2)^2 - (\mathbf{v}_1 \times \mathbf{v}_2)^2}. \quad (6.23)$$

In various physical setups, most notably in astrophysics, one needs to compute the cross sections *measured by a generic observer* with respect to whom the momenta of the colliding particles form an arbitrary angle. This requires the evaluation of the denominator in Eq. (6.18) in a generic “oblique” frame,

$$F_{\text{obl}} = 4E_1 E_2 |\mathbf{v}_1 - \mathbf{v}_2| = 4|E_2 \mathbf{p}_1 - E_1 \mathbf{p}_2|. \quad (6.24)$$

To relate  $F_{\text{obl}}$  to the corresponding factor for the collinear observer,  $F_{\text{coll}}$ , we split the incoming momenta into their components parallel and perpendicular to the center of mass momentum  $\mathbf{P}_{\text{cm}} = \mathbf{p}_1 + \mathbf{p}_2$ ,

$$\mathbf{p}_{i\parallel} = \left( \frac{\mathbf{p}_i \cdot \mathbf{P}_{\text{cm}}}{\mathbf{P}_{\text{cm}}^2} \right) \mathbf{P}_{\text{cm}}, \quad \mathbf{p}_{i\perp} = \mathbf{p}_i - \mathbf{p}_{i\parallel}, \quad (6.25)$$

with  $i = 1, 2$ . It is not difficult to show that  $\mathbf{p}_{1\perp} = -\mathbf{p}_{2\perp} \equiv \mathbf{p}_\perp$ . Applying now this decomposition to Eq. (6.24) we arrive at

$$F_{\text{obl}} = 4\sqrt{(E_2\mathbf{p}_{1\parallel} - E_1\mathbf{p}_{2\parallel})^2 + (E_1 + E_2)^2\mathbf{p}_\perp^2}. \quad (6.26)$$

To go from the oblique frame to the center of mass frame, we only have to perform a boost with velocity

$$\mathbf{V} = \frac{1}{E_1 + E_2}\mathbf{P}_{\text{cm}}. \quad (6.27)$$

This boost only transforms the parallel components of the momenta,  $\mathbf{p}_{i\parallel}$ . It is possible to show that the combination  $E_2\mathbf{p}_{1\parallel} - E_1\mathbf{p}_{2\parallel}$  appearing under the square root in Eq. (6.26) is left invariant by the boost. Hence, it can be computed either in the oblique or the center of mass frame and consequently we can write

$$F_{\text{obl}}^2 = F_{\text{coll}}^2 + 16\left[(E_1 + E_2)^2 - (E_1^{\text{cm}} + E_2^{\text{cm}})^2\right]\mathbf{p}_\perp^2, \quad (6.28)$$

where we have used superscripts to indicate the quantities that are referred to the center of mass frame. Finally, we notice that the second term inside the square brackets is just the Lorentz invariant quantity  $(p_1 + p_2)^2$ . Evaluating it in the oblique frame we arrive at the final expression

$$F_{\text{obl}}^2 = F_{\text{coll}}^2 + 16\mathbf{p}_\perp^2\mathbf{P}_{\text{cm}}^2. \quad (6.29)$$

We have seen that in a collision experiment all collinear observers measure the same value of the cross section.<sup>2</sup> This is not the case, however, for the cross section measured by another observer boosted with respect to the collinear ones along a direction forming a non-zero angle with the beams. In this oblique frame, both  $\mathbf{P}_{\text{cm}}$  and  $\mathbf{p}_\perp$  are different from zero and from Eq. (6.29) the cross section is suppressed by a larger value in the denominator. This can be understood heuristically by thinking that, as the result of this transverse boost, the area of the sections normal to the beams are Lorentz contracted.

We have learned how particle cross sections are given in terms of the invariant amplitude for the corresponding processes, which in turn are related to the  $S$ -matrix amplitudes. Generically, an *exact* computation of these amplitudes in quantum field theory is not feasible. Nevertheless, in many physical situations it can be argued that interactions are weak enough to allow for a perturbative evaluation. In the remainder of this chapter we will describe how  $S$ -matrix elements can be computed in perturbation theory using Feynman diagrams and rules. These are very convenient book-keeping techniques allowing both to track all contributions to a process at a given order in perturbation theory and to compute them.

---

<sup>2</sup> This is a particular case of Eq. (6.29) where  $\mathbf{p}_\perp = 0$  for all collinear observers.



## 6.2 From Green's Functions to Scattering Amplitudes

The basic quantities to be computed in quantum field theory are the vacuum expectation values of products of the operators of the theory. Particularly useful are time-ordered Green's functions of a number of local operators  $\mathcal{O}_i(x)$

$$\langle \Omega | T \left[ \mathcal{O}_1(x_1) \dots \mathcal{O}_n(x_n) \right] | \Omega \rangle, \quad (6.30)$$

where  $|\Omega\rangle$  is the ground state of the theory and the time ordered product has been defined in Eq. (2.63).

The interest of these correlation functions lies in the fact that they can be related to  $S$ -matrix amplitudes through the so-called reduction formula. The idea consists of replacing a particle of momentum  $\mathbf{p}$  in the in- or out-state by the insertion of a certain quantum field  $\phi(x)$  interpolating between the vacuum and the one-particle states with the normalization

$$\langle \Omega | \phi(t, \mathbf{x}) | p \rangle = \varphi(\mathbf{p}) e^{-iE_{\mathbf{p}}t + i\mathbf{p}\cdot\mathbf{x}}, \quad (6.31)$$

where  $\varphi(\mathbf{p})$  is the one-particle wave function, carrying the corresponding indices and quantum numbers: for example,  $\varphi = 1$  for a scalar field while  $\varphi = \varepsilon_{\mu}(\mathbf{p}, \lambda)$  for the electromagnetic field.<sup>3</sup> This expression fixes the global normalization of the field, while the coordinate dependence is completely determined by the translational invariance of the vacuum state  $|\Omega\rangle$  [see Eq. (2.36)].

To keep our discussion as simple as possible, we will not derive the reduction formula, or even write it down in full detail. Suffice it to say that the reduction formula states that any  $S$ -matrix amplitude

$$\langle p'_1, \dots, p'_k; \text{out} | p_1, \dots, p_n; \text{in} \rangle \quad (6.32)$$

can be written in terms of the Fourier transform of a time-ordered correlation function

$$\int d^4x_1 \dots d^4x_k \int d^4y_1 \dots d^4y_n \langle \Omega | T \left[ \phi(x_1)^\dagger \dots \phi(x_k)^\dagger \phi(y_1) \dots \phi(y_n) \right] | \Omega \rangle \times e^{ip'_1 \cdot x_1 + \dots + ip'_k \cdot x_k} e^{-ip_1 \cdot y_1 - \dots - ip_n \cdot y_n}, \quad (6.33)$$

where  $\phi(x)$  is a field that “creates” the particles out of the vacuum. Since the momenta of the particles in the asymptotic states are on-shell, the expression (6.33) has to be evaluated in the limit  $p_i^2, p_j^2 \rightarrow m^2$ , where it diverges. In the reduction formula connecting (6.32) with (6.33) these poles are cancelled by factors of

<sup>3</sup> The field  $\phi(x)$  appearing in Eq. (6.31) is the so-called “renormalized” field, and it is not canonically normalized. It is related to the canonically normalized “bare” field  $\phi_0(x)$  by an overall numerical factor,  $\phi_0(x) = \sqrt{Z_\phi} \phi(x)$ , where  $Z_\phi = 1$  in the case of a free field. The difference between bare and renormalized fields will become clear in Chap. 8 (see Sect. 8.3).

$p_i^2 - m^2$  and  $p_j^2 - m^2$ . The technical details and the form taken by the reduction formula for various quantum field theories can be found in the textbooks listed in Ref. [1–15] of [Chap. 1](#).

The “interpolating field” used to write the scattering amplitude in terms of Green’s functions is not uniquely determined. Any local field satisfying the normalization Eq. (6.31) can be used for this purpose. The scattering amplitudes calculated from a quantum field theory are invariant under local field redefinitions. For example, for a massive field  $\phi(x)$  we could use in Eq. (6.33) instead of  $\phi(x)$  the local field

$$\phi'(x) = -\frac{1}{m^2} \square \phi(x) \quad (6.34)$$

that also interpolates between the one-particle states and the vacuum with the correct normalization (6.31).

### 6.3 Feynman Rules

The reduction formula transforms the problem of computing  $S$ -matrix elements to the evaluation of time-ordered correlation functions. These quantities are easy to compute exactly for free fields. For an interacting theory, generically we can only evaluate them perturbatively. Using path integrals, the vacuum expectation value of the time-ordered product of a number of operators can be written as

$$\langle \Omega | T \left[ \mathcal{O}_1(x_1) \dots \mathcal{O}_n(x_n) \right] | \Omega \rangle = \frac{\int \mathcal{D}\phi \mathcal{D}\phi^\dagger \mathcal{O}_1(x_1) \dots \mathcal{O}_n(x_n) e^{iS[\phi, \phi^\dagger]}}{\int \mathcal{D}\phi \mathcal{D}\phi^\dagger e^{iS[\phi, \phi^\dagger]}}. \quad (6.35)$$

For a theory with interactions, neither the path integral in the numerator or in the denominator are Gaussian and cannot be computed exactly. In spite of this, Eq. (6.35) is still very useful to implement a perturbative calculation. The action  $S[\phi, \phi^\dagger]$  can be split into the free (quadratic) and the interaction parts

$$S[\phi, \phi^\dagger] = S_0[\phi, \phi^\dagger] + S_{\text{int}}[\phi, \phi^\dagger]. \quad (6.36)$$

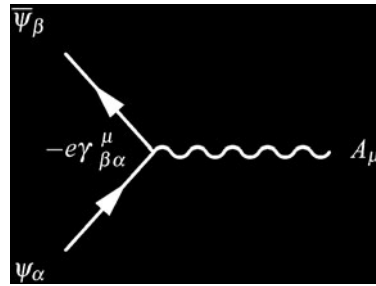
All dependence on the coupling constants of the theory comes from the second piece. Expanding  $\exp(iS_{\text{int}})$  in power series of the coupling, we find that each term in the series expansion of the integrals in Eq. (6.35) has the following structure

$$\int \mathcal{D}\phi \mathcal{D}\phi^\dagger [\dots] e^{iS_0[\phi, \phi^\dagger]}, \quad (6.37)$$

where “[...]” denotes certain monomial of fields.

The crucial point is that the integration measure  $\mathcal{D}\phi \mathcal{D}\phi^\dagger \exp(iS_0)$  only involves the free action, so the path integrals (6.37) are Gaussian and therefore can be computed exactly. The same conclusion can be reached using the operator formalism.



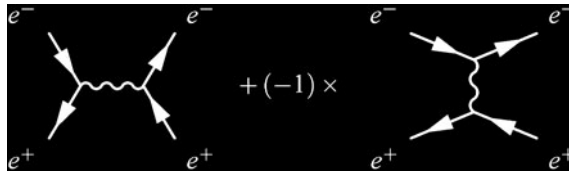


To compute an  $S$ -matrix amplitude to a given order in  $e$ , one should draw all possible diagrams with as many vertices as the order in perturbation theory, and the number and type of external legs dictated by the in and out states of the amplitude. It is very important to keep in mind that in joining the fermion lines among the different building blocks of the diagram one has to respect their orientation. This reflects the conservation of the electric charge. In addition, one should only consider diagrams that are topologically non-equivalent, i.e. that cannot be smoothly deformed into one another while keeping the external legs fixed.<sup>4</sup>

To show practically how Feynman diagrams are drawn, we consider Bhabha scattering: elastic electron–positron scattering

$$e^+ + e^- \longrightarrow e^+ + e^-.$$

Our problem is to compute the  $S$ -matrix amplitude to leading order in the electric charge. Since the QED vertex contains a photon line and our process does not have photons in the initial or the final states, drawing a Feynman diagram requires at least two vertices. In fact, the leading contribution is of order  $e^2$  and comes from the following two diagrams



Incoming and outgoing particles appear respectively on the left and the right of these diagrams. The identification of electrons and positrons is done by comparing the direction of the charge flux with the direction of propagation. For electrons the flux of charge goes in the direction of propagation, whereas for positrons they go in

<sup>4</sup> From the point of view of the operator formalism, the requirement of considering only diagrams that are topologically nonequivalent comes from the fact that each diagram represents a certain Wick contraction in the correlation function of interaction–picture operators.

opposite directions. These are the only two diagrams that can be drawn to this order in perturbation theory.

It should be noticed that the two diagrams contribute with opposite signs. The reason is that the second diagram can be obtained from the first one by interchanging the incoming positron external line attached to the vertex on the left with that of the outgoing electron coming from the vertex on the right. This permutation of two fermions introduces the minus sign.

We have learned how to draw Feynman diagrams in QED. Now it is time to compute the contribution of each one to the amplitude using the Feynman rules. The idea is simple: each of the diagram's building blocks (vertices as well as external and internal lines) comes associated with a term. Putting all of them together according to certain rules results in the contribution of the corresponding diagram to the amplitude. In the case of QED in the Feynman gauge ( $\xi = 1$ ), we have the following correspondence for vertices and internal propagators:

$$\begin{aligned} \alpha \longrightarrow \beta &\implies \left( \frac{i}{\not{p} - m + i\epsilon} \right)_{\beta\alpha} \\ \mu \text{ wavy } \nu &\implies \frac{-i\eta_{\mu\nu}}{p^2 + i\epsilon} \\ \begin{array}{c} \beta \\ \nearrow \\ \alpha \end{array} \text{ wavy } \mu &\implies -ie\gamma_{\beta\alpha}^{\mu} \end{aligned}$$

In addition, each vertex carries a factor  $(2\pi)^4 \delta^{(4)}(p_1 + p_2 + p_3)$  implementing momentum conservation, where we take the convention that all momenta are entering the vertex. The Feynman rules for other values of the gauge fixing parameter  $\xi$  only differ from the ones above by an extra term in the photon propagator. In addition, one has to perform an integration over the momenta running in internal lines with the measure

$$\int \frac{d^4 p}{(2\pi)^4}, \quad (6.42)$$

and introduce a factor of  $-1$  for each fermion loop in the diagram.<sup>5</sup>

<sup>5</sup> The contribution of each diagram comes also multiplied by a symmetry factor that takes into account in how many ways a given Wick contraction can be done. In QED, however, these factors are equal to one for many diagrams.

A number of integrations over the internal momenta can be eliminated using the delta functions from the vertices. The result is a global delta function implementing the total momentum conservation in the diagram [cf. Eq. (6.8)]. In fact, there is a whole class of diagrams for which *all* integrations can be eliminated in this way. These are the so-called tree level diagrams containing no closed loops. As a general rule, there will be as many remaining integrations as the number of independent loops in the diagram.

Generically, finding the contribution of a Feynman diagram with  $\ell$  independent loops involves the calculation of integrals of the form

$$I(p_1, \dots, p_n) = \int \frac{d^4 q_1}{(2\pi)^4} \dots \frac{d^4 q_\ell}{(2\pi)^4} f(q_1, \dots, q_\ell; p_1, \dots, p_n), \quad (6.43)$$

where  $f(q_1, \dots, q_\ell; p_1, \dots, p_n)$  is a rational function of its arguments and  $p_1, \dots, p_n$  are the external momenta. In many cases these integrals are divergent. When the divergence is associated with the limit of small loop momenta it is called an *infrared divergence*. They usually cancel once all diagrams contributing to a given order in perturbation theory are added together. The second type of divergences that one expects in the integrals (6.43) comes from the region of large loop momenta. These are called *ultraviolet divergences*. They cannot be cancelled by adding the contribution of different diagram and have to be dealt with using the procedure of renormalization. We will discuss this problem in some detail in [Chaps. 8](#) and [12](#).


This is not the end of the story. In the calculation of  $S$ -matrix amplitudes the contribution of the Feynman diagram contains factors associated with the external legs. These are the wave functions and/or polarization tensor of the corresponding asymptotic states containing all the information about the spin and polarization of the incoming and outgoing particles. In the case of QED these factors are:


Incoming fermion:  $\alpha \rightarrow \text{circle with diagonal lines} \Rightarrow u_\alpha(\mathbf{p}, s)$

Incoming antifermion:  $\alpha \leftarrow \text{circle with diagonal lines} \Rightarrow \bar{v}_\alpha(\mathbf{p}, s)$

Outgoing fermion:  $\text{circle with diagonal lines} \rightarrow \alpha \Rightarrow \bar{u}_\alpha(\mathbf{p}, s)$

Outgoing antifermion:  $\text{circle with diagonal lines} \leftarrow \alpha \Rightarrow v_\alpha(\mathbf{p}, s)$

Incoming photon:  $\mu$    $\Rightarrow \epsilon_\mu(\mathbf{p})$

Outgoing photon:   $\mu \Rightarrow \epsilon_\mu(\mathbf{p})^*$

Here  $u_\alpha(\mathbf{p}, s)$ ,  $v_\alpha(\mathbf{p}, s)$  are the positive and negative energy solutions of the Dirac equation introduced in [Chap. 3](#), whereas  $\epsilon_\mu(\mathbf{p}, \lambda)$  is the polarization tensor of the photon with polarization  $\lambda$ . Here we have assumed that the momenta for incoming (resp. outgoing) particles are entering (resp. leaving) the diagram, and all external momenta are on-shell,  $p_i^2 = m_i^2$ .

The use of Feynman diagrams is not restricted to quantum field theory, they can also be found in condensed matter physics and statistical mechanics. Their calculation is not an easy task. The number of diagrams contributing to a process grows very fast with the order of perturbation theory and the integrals arising in calculating loop diagrams soon get very complicated.

Feynman rules can be constructed for any interacting quantum field theory with scalar, vector or spinor fields. For the nonabelian gauge theories introduced in [Chap. 4](#) these are:

$$\begin{aligned} \alpha, i \longrightarrow \beta, j &\Rightarrow \left( \frac{i}{\not{p} - m + i\epsilon} \right)_{\beta\alpha} \delta_{ij} \\ \mu, A \text{ (wavy)} \text{ } \nu, B &\Rightarrow \frac{-i\eta_{\mu\nu}}{p^2 + i\epsilon} \delta^{AB} \\ \begin{array}{l} \beta, j \\ \alpha, i \end{array} \text{ (arrows)} \text{ } \nu, B \text{ (wavy)} &\Rightarrow -ig\gamma_{\beta\alpha}^\mu t_{ij}^A \end{aligned}$$

$$\begin{array}{l} \sigma, C \text{ (wavy)} \\ \nu, B \text{ (wavy)} \end{array} \text{ } \mu, A \text{ (wavy)} \Rightarrow g f^{ABC} \left[ \eta^{\mu\nu} (p_1^\sigma - p_2^\sigma) + \text{permutations} \right]$$

$$\Rightarrow -ig^2 [f^{ABE} f^{CDE} (\eta^{\mu\sigma} \eta^{\nu\lambda} - \eta^{\mu\lambda} \eta^{\nu\sigma}) + \text{permutations}]$$

As in the case of QED, each vertex includes a delta function implementing momentum conservation.

It is not our aim here to give a full and detailed description of the Feynman rules for nonabelian gauge theories. We only point out that, unlike the case of QED, here the gauge fields interact among themselves. These three and four gauge field vertices are a consequence of the cubic and quartic terms in the Lagrangian (4.54). The self-interactions of the nonabelian gauge field theories have crucial dynamical consequences and its at the very heart of their physical successes.

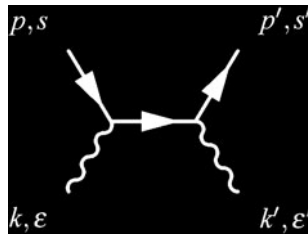
## 6.4 An Example: Compton Scattering at Low Energies

We illustrate now the use of Feynman diagrams in the calculation of observables in physical processes by studying an example with important physical applications. This is the calculation of the cross section for the dispersion of photons by free electrons: Compton scattering

$$\gamma(k, \varepsilon) + e^-(p, s) \longrightarrow \gamma(k', \varepsilon') + e^-(p', s'). \quad (6.44)$$

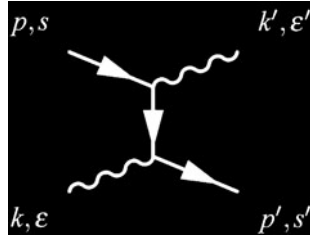
Inside the parenthesis we have indicated the momenta for the different particles, as well as the polarizations and spins of the incoming and outgoing photons and electrons respectively. We study this scattering in the nonrelativistic limit for the electrons.

The first step in our calculation is to identify all the diagrams contributing to (6.44) at leading order. Since the vertex of QED contains two fermion and one photon leg it is immediate to realize that any diagram contributing to this process must contain at least two vertices, so the leading contribution is of order  $e^2$ . A first diagram that can be drawn is:





There is however a second possibility given by the following diagram:



These two diagrams are topologically nonequivalent, since deforming one into the other requires changing the label of the external legs. In addition, unlike the example of the Bhabha scattering studied in the previous section, both diagrams contribute with the same sign. This is because they are related by interchanging the incoming with the outgoing photon. Since photons are bosons, no minus sign comes from this permutation.

Using the Feynman rules of QED we find the contribution of the two diagrams to be

$$\begin{aligned}
 & \text{Diagram 1} + \text{Diagram 2} \\
 &= (ie)^2 \bar{u}(\mathbf{p}', s') \not{\epsilon}'(\mathbf{k}')^* \frac{\not{p} + \not{k} + m_e}{(p+k)^2 - m_e^2} \not{\epsilon}(\mathbf{k}) u(\mathbf{p}, s) \\
 &+ (ie)^2 \bar{u}(\mathbf{p}', s') \not{\epsilon}(\mathbf{k}) \frac{\not{p} - \not{k}' + m_e}{(p-k')^2 - m_e^2} \not{\epsilon}'(\mathbf{k}')^* u(\mathbf{p}, s).
 \end{aligned} \tag{6.45}$$

where  $m_e$  is the electron mass and we have factored out  $(2\pi)^4$  times the delta function implementing momentum conservation. As explained in [Sect. 6.3](#), all incoming and outgoing particles are on-shell,

$$p^2 = m_e^2 = p'^2 \quad \text{and} \quad k^2 = 0 = k'^2. \tag{6.46}$$

Our calculation involves only tree-level diagrams, so there is no integration left over internal momenta. To get an explicit result we begin by simplifying the numerators. The following simple identity turns out to be very useful

$$\not{a} \not{b} = -\not{b} \not{a} + 2(a \cdot b) \mathbf{1}. \tag{6.47}$$

In addition, we are interested in Compton scattering at low energy when electrons are nonrelativistic particles. This is known in the literature as Thomson scattering. To be more precise, we take all spatial momenta much smaller than the electron mass

$$|\mathbf{p}|, |\mathbf{k}|, |\mathbf{p}'|, |\mathbf{k}'| \ll m_e. \tag{6.48}$$

In this approximation, the amplitude for Compton scattering simplifies substantially. Let us begin with the first term in Eq. (6.45). Applying the identity (6.47) we obtain

$$(\not{p} + \not{k} + m_e)\not{\epsilon}(\mathbf{k})u(\mathbf{p}, s) = -\not{\epsilon}(\mathbf{k})(\not{p} - m_e)u(\mathbf{p}, s) + \not{k}\not{\epsilon}(\mathbf{k})u(\mathbf{p}, s) + 2p \cdot \epsilon(\mathbf{k})u(\mathbf{p}, s). \quad (6.49)$$

The first term on the right-hand side of this equation vanishes using Eq. (3.45). Moreover, in the approximation (6.48) we find that the electrons' four-momenta can be written  $p^\mu, p'^\mu \approx (m_e, 0)$  and therefore

$$p \cdot \epsilon(\mathbf{k}) = 0. \quad (6.50)$$

This follows from the absence of the temporal photon polarization,  $\epsilon^0(\mathbf{k}) = 0$ . Thus, we conclude that at low energies

$$(\not{p} + \not{k} + m_e)\not{\epsilon}(\mathbf{k})u(\mathbf{p}, s) = \not{k}\not{\epsilon}(\mathbf{k})u(\mathbf{p}, s) \quad (6.51)$$

and similarly for the second term in Eq. (6.45)

$$(\not{p} - \not{k}' + m_e)\not{\epsilon}'(\mathbf{k}')^*u(\mathbf{p}, s) = -\not{k}'\not{\epsilon}'(\mathbf{k}')^*u(\mathbf{p}, s). \quad (6.52)$$

Next, we turn to the denominators in (6.45). Using the mass-shell condition we find

$$\begin{aligned} (p+k)^2 - m_e^2 &= p^2 + k^2 + 2p \cdot k - m_e^2 = 2p \cdot k \\ &= 2\omega_p|\mathbf{k}| - 2\mathbf{p} \cdot \mathbf{k} \end{aligned} \quad (6.53)$$


and

$$\begin{aligned} (p-k')^2 - m_e^2 &= p^2 + k'^2 + 2p \cdot k' - m_e^2 = -2p \cdot k' \\ &= -2\omega_p|\mathbf{k}'| + 2\mathbf{p} \cdot \mathbf{k}'. \end{aligned} \quad (6.54)$$

Working again in the low energy approximation (6.48), these two expressions simplify to

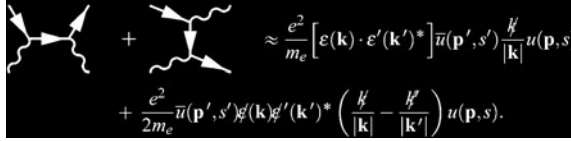
$$(p+k)^2 - m_e^2 \approx 2m_e|\mathbf{k}|, \quad (p-k')^2 - m_e^2 \approx -2m_e|\mathbf{k}'|. \quad (6.55)$$

Collecting all results we obtain



$$\approx \frac{(ie)^2}{2m_e} \bar{u}(\mathbf{p}', s') \left[ \not{\epsilon}'(\mathbf{k}')^* \frac{\not{k}}{|\mathbf{k}|} \epsilon(\mathbf{k}) + \epsilon(\mathbf{k}) \frac{\not{k}'}{|\mathbf{k}'|} \not{\epsilon}'(\mathbf{k}')^* \right] u(\mathbf{p}, s). \quad (6.56)$$

Using the identity (6.47) a number of times, as well as the transversality condition of the polarization vectors (4.32), we end up with a simpler expression



$$\begin{aligned}
& \approx \frac{e^2}{m_e} [\boldsymbol{\varepsilon}(\mathbf{k}) \cdot \boldsymbol{\varepsilon}'(\mathbf{k}')^*] \bar{u}(\mathbf{p}', s') \frac{\not{k}}{|\mathbf{k}|} u(\mathbf{p}, s) \\
& + \frac{e^2}{2m_e} \bar{u}(\mathbf{p}', s') \not{\boldsymbol{\varepsilon}}(\mathbf{k}) \not{\boldsymbol{\varepsilon}}'(\mathbf{k}')^* \left( \frac{\not{k}}{|\mathbf{k}|} - \frac{\not{k}'}{|\mathbf{k}'|} \right) u(\mathbf{p}, s).
\end{aligned} \tag{6.57}$$

With a little extra effort one can show that the second term on the right-hand side of this equation vanishes. First we notice that in the low energy limit  $|\mathbf{k}| \approx |\mathbf{k}'|$ . If, in addition, we use the conservation of momentum  $k - k' = p' - p$  and the identity (3.45) we can write

$$\bar{u}(\mathbf{p}', s') \not{\boldsymbol{\varepsilon}}(\mathbf{k}) \not{\boldsymbol{\varepsilon}}'(\mathbf{k}')^* \left( \frac{\not{k}}{|\mathbf{k}|} - \frac{\not{k}'}{|\mathbf{k}'|} \right) u(\mathbf{p}, s) \approx \frac{1}{|\mathbf{k}|} \bar{u}(\mathbf{p}', s') \not{\boldsymbol{\varepsilon}}(\mathbf{k}) \not{\boldsymbol{\varepsilon}}'(\mathbf{k}')^* (\not{p}' - m_e) u(\mathbf{p}, s). \tag{6.58}$$

Next we use the identity (6.47) to take the term  $(\not{p}' - m_e)$  to the right. Finally, keeping in mind that in the low energy limit the electron four-momenta are orthogonal to the photon polarization vectors [see Eq. (6.50)], we conclude that

$$\bar{u}(\mathbf{p}', s') \not{\boldsymbol{\varepsilon}}(\mathbf{k}) \not{\boldsymbol{\varepsilon}}'(\mathbf{k}')^* (\not{p}' - m_e) u(\mathbf{p}, s) = \bar{u}(\mathbf{p}', s') (\not{p}' - m_e) \not{\boldsymbol{\varepsilon}}(\mathbf{k}) \not{\boldsymbol{\varepsilon}}'(\mathbf{k}')^* u(\mathbf{p}, s) = 0 \tag{6.59}$$

where the last identity follows from the equation satisfied by the conjugate positive-energy spinor,  $\bar{u}(\mathbf{p}', s') (\not{p}' - m_e) = 0$ .

After all these lengthy manipulations we have finally arrived at the expression of the invariant amplitude for the Compton scattering at low energies

$$i\mathcal{M}_{i \rightarrow f} = \frac{e^2}{m_e} [\boldsymbol{\varepsilon}(\mathbf{k}) \cdot \boldsymbol{\varepsilon}'(\mathbf{k}')^*] \bar{u}(\mathbf{p}', s') \frac{\not{k}}{|\mathbf{k}|} u(\mathbf{p}, s). \tag{6.60}$$

To calculate the cross section we need to compute  $|\mathcal{M}_{i \rightarrow f}|^2$ , as shown in Eq. (6.18). For many physical applications, however, one is interested in the dispersion of photons with a given polarization by electrons that are not polarized, i.e. whose spins are randomly distributed. To describe this physical setup we have to average over initial electron polarization (since we do not know them) and sum over all possible final electron polarization (because our detector is blind to this quantum number),

$$\overline{|i\mathcal{M}_{i \rightarrow f}|^2} = \frac{1}{2} \left( \frac{e^2}{m_e |\mathbf{k}|} \right)^2 |\boldsymbol{\varepsilon}(\mathbf{k}) \cdot \boldsymbol{\varepsilon}'(\mathbf{k}')^*|^2 \sum_{s=\pm\frac{1}{2}} \sum_{s'=\pm\frac{1}{2}} |\bar{u}(\mathbf{p}', s') \not{k} u(\mathbf{p}, s)|^2. \tag{6.61}$$

The factor of  $\frac{1}{2}$  comes from averaging over the two possible polarizations of the incoming electrons. The sums in this expression can be calculated without much difficulty. Expanding the absolute value

$$\sum_{s=\pm\frac{1}{2}} \sum_{s'=\pm\frac{1}{2}} |\bar{u}(\mathbf{p}', s') \not{k} u(\mathbf{p}, s)|^2 = \sum_{s=\pm\frac{1}{2}} \sum_{s'=\pm\frac{1}{2}} \left[ u(\mathbf{p}, s)^\dagger \not{k}^\dagger \bar{u}(\mathbf{p}', s')^\dagger \right] \left[ \bar{u}(\mathbf{p}', s') \not{k} u(\mathbf{p}, s) \right], \quad (6.62)$$

and using that  $\gamma^{\mu\dagger} = \gamma^0 \gamma^\mu \gamma^0$  one finds, after some manipulations,

$$\begin{aligned} \sum_{s=\pm\frac{1}{2}} \sum_{s'=\pm\frac{1}{2}} |\bar{u}(\mathbf{p}', s') \not{k} u(\mathbf{p}, s)|^2 &= \left[ \sum_{s=\pm\frac{1}{2}} u_\alpha(\mathbf{p}, s) \bar{u}_\beta(\mathbf{p}, s) \right] (\not{k})_{\beta\sigma} \left[ \sum_{s'=\pm\frac{1}{2}} u_\sigma(\mathbf{p}', s') \bar{u}_\rho(\mathbf{p}', s') \right] (\not{k})_{\rho\alpha} \\ &= \text{Tr} [(\not{p} + m_e) \not{k} (\not{p}' + m_e) \not{k}], \end{aligned} \quad (6.63)$$

where the final result has been obtained using the completeness relations (3.51). The final evaluation of the trace can be done using the relation (6.47) to commute  $\not{p}'$  and  $\not{k}$ . Using  $k^2 = 0$  and that we are working in the low energy limit, we have<sup>6</sup>

$$\text{Tr} [(\not{p} + m_e) \not{k} (\not{p}' + m_e) \not{k}] = 2(p \cdot k)(p' \cdot k) \text{Tr} \mathbf{1} \approx 8m_e^2 |\mathbf{k}|^2. \quad (6.64)$$

With this we arrive at the following value for the invariant amplitude for the Compton scattering at low energies

$$\overline{|i\mathcal{M}_{i \rightarrow f}|^2} = 4e^4 |\boldsymbol{\varepsilon}(\mathbf{k}) \cdot \boldsymbol{\varepsilon}'(\mathbf{k}')^*|^2. \quad (6.65)$$

We have reached the end of our calculation. Plugging  $\overline{|i\mathcal{M}_{i \rightarrow f}|^2}$  into (6.22) and dropping the integration over the direction of the outgoing particles we find the differential cross section for the scattering of a photon by an electron at rest

$$\frac{d\sigma}{d\Omega} = \frac{1}{64\pi^2 m_e^2} \overline{|i\mathcal{M}_{i \rightarrow f}|^2} = \left( \frac{e^2}{4\pi m_e} \right)^2 |\boldsymbol{\varepsilon}(\mathbf{k}) \cdot \boldsymbol{\varepsilon}'(\mathbf{k}')^*|^2. \quad (6.66)$$

The prefactor of the last expression is precisely the square of the classical electron radius  $r_{\text{cl}}$ . In fact, the result can be rewritten as

$$\frac{d\sigma}{d\Omega} = \frac{3}{8\pi} \sigma_T |\boldsymbol{\varepsilon}(\mathbf{k}) \cdot \boldsymbol{\varepsilon}'(\mathbf{k}')^*|^2, \quad (6.67)$$

where  $\sigma_T$  is the total Thomson cross section

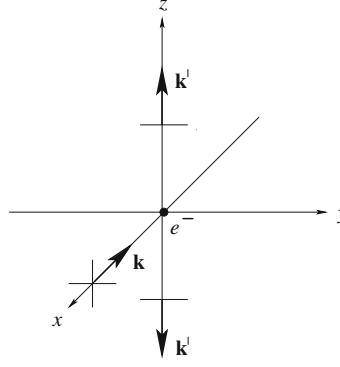
$$\sigma_T = \frac{e^4}{6\pi m_e^2} = \frac{8\pi}{3} r_{\text{cl}}^2, \quad (6.68)$$

obtained from integrating (6.66) over angles.

One of the most important physical consequences of Eq. (6.67) is that a net polarization is produced in the scattering of unpolarized radiation off nonrelativistic charges. To see this, we take the Thomson differential cross section and average over

<sup>6</sup> We use also the fact that the trace of the product of an odd number of Dirac matrices is always zero.

**Fig. 6.2** This figure illustrate Eq. (6.70). The “vertical” component of the unpolarized radiation arriving from the  $x$  direction is suppressed in the photons scattered along the  $z$  axis. This results in a linear polarization of the scattered radiation



the polarization of the incoming photon. Denoting by  $\varepsilon(\mathbf{k}, a)$ , with  $a = 1, 2$ , a basis for the photon polarizations, this average gives

$$\frac{1}{2} \sum_{a=1,2} |\varepsilon(\mathbf{k}, a) \cdot \varepsilon'(\mathbf{k}')^*|^2 = \left[ \frac{1}{2} \sum_{a=1,2} \varepsilon_i(\mathbf{k}, a) \varepsilon_j(\mathbf{k}, a)^* \right] \varepsilon_j(\mathbf{k}') \varepsilon_i(\mathbf{k}')^*. \quad (6.69)$$

The sum inside the brackets can be computed using the normalization of the polarization vectors,  $|\varepsilon(\mathbf{k}, n)|^2 = 1$ , and the transversality condition  $\mathbf{k} \cdot \varepsilon(\mathbf{k}, n) = 0$

$$\begin{aligned} \frac{1}{2} \sum_{a=1,2} |\varepsilon(\mathbf{k}, a) \cdot \varepsilon'(\mathbf{k}')^*|^2 &= \frac{1}{2} \left( \delta_{ij} - \frac{k_i k_j}{|\mathbf{k}|^2} \right) \varepsilon'_j(\mathbf{k}') \varepsilon'_i(\mathbf{k}')^* \\ &= \frac{1}{2} \left[ 1 - |\hat{\mathbf{k}} \cdot \varepsilon'(\mathbf{k}')|^2 \right], \end{aligned} \quad (6.70)$$

where  $\hat{\mathbf{k}} = \frac{\mathbf{k}}{|\mathbf{k}|}$  is the unit vector in the direction of the incoming photon.

From the last equation we conclude that Thomson scattering suppresses all polarizations parallel to the direction of the incoming photon. At the same time, the differential cross section reaches its maximum values when the polarization of the scattered photon lies in the plane normal to  $\hat{\mathbf{k}}$ . This is represented in Fig. 6.2, where nonpolarized radiation coming from the  $x$  direction is scattered by a nonrelativistic electron. According to Eq. (6.70) the vertical polarization is fully suppressed in the radiation scattered along the  $z$  direction, thus producing linear polarization.

## 6.5 Polarization of the Cosmic Microwave Background Radiation

The differential cross section of Thomson scattering we have derived is relevant in many areas of physics, but its importance is paramount in the study of the cosmological microwave background radiation (CMB). Here we are going to review briefly

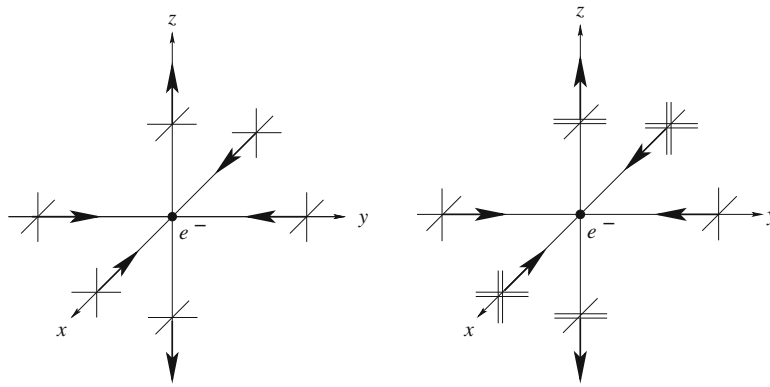


**Fig. 6.3** In these figures the larger density of unpolarized photons arriving from different directions is represented through two parallel lines indicating the polarization. The *left panel* shows the scattering of isotropic radiation by a free electron and how this does not produce any net polarization in the scattered photons. On the *right panel*, on the other hand, the anisotropy in the intensity of the radiation has a quadrupole component, being larger along the  $x$  direction. The result is a net polarization in the photons scattered along the  $z$  axis

how polarization emerges in the cosmic radiation and discuss why its detection could serve as a window to the physics of the very early universe. Our presentation will be rather sketchy. A thorough analysis of this problem can be found in many places, such as [1, 2].

Just before recombination the universe is filled with a plasma of electrons interacting with photons via Compton scattering. This plasma has a temperature of the order of  $T \approx 1$  keV and therefore electrons are nonrelativistic ( $T \ll m_e \sim 0.5$  MeV), so the approximations leading to the Thomson differential cross section apply. At the last scattering surface there is no way to know the polarization state of the photons in the plasma before they are scattered by electrons to produce the CMB radiation that we detect today. Therefore we have to average over incoming polarizations as shown at the end of the previous section.

The relation between the polarization of the CMB and the anisotropies in the density of photons at last scattering can be understood with the help of Fig. 6.2. We consider the polarization of photons traveling along the  $z$  direction resulting from the scattering of photons traveling along the  $x$  and  $y$  axis. Since Thomson scattering suppresses all polarizations in the direction of the incoming photons we find that the two polarizations in the scattered radiation come from the “horizontal” polarizations of the incoming photons. If the number of photons coming from the  $x$  and  $y$  directions are the same no net polarization is produced. This is shown in the left panel of Fig. 6.3. It is an instructive exercise to check that no polarization is produced either in the presence of a dipolar anisotropy.

When the anisotropy has a quadrupole component, on the other hand, the situation changes. Then the intensity of the unpolarized radiation approaching from the  $x$  and

y directions is different and so is the relative intensity of the two polarizations in the scattered radiation along the  $z$  axis. The outgoing radiation is then polarized.

The previous heuristic arguments show that the presence of a net polarization in the CMB is the smoking gun of quadrupole anisotropies in the photon distribution at the last scattering surface. There are several possible physical causes for such an anisotropy. One of them, however, is specially glaring. Gravitational waves propagating through the plasma induce changes in its density with precisely the quadrupole component necessary to produce the polarization in the CMB radiation.

Now we make this discussion more precise. The polarization of radiation can be described using three Stokes parameters:  $Q$  measures the excess of horizontal versus vertical,  $U$  of diagonal versus antidiagonal and  $V$  of left versus right polarization. CMB experiments allow the measurements of these parameters for the background radiation arriving from a direction in the sky specified by a unit vector  $\hat{\mathbf{n}}$ .

To compute the parameter  $Q(\hat{\mathbf{n}})$  we consider the polarizations along the directions defined by the unit vectors  $\hat{\mathbf{e}}_{\leftrightarrow} = -\hat{\mathbf{e}}_{\varphi}$  and  $\hat{\mathbf{e}}_{\updownarrow} = -\hat{\mathbf{e}}_{\theta}$ , normal to the plane defined by  $\hat{\mathbf{n}}$  (see left panel in Fig. 6.4). We denote by  $f(\hat{\mathbf{k}}, \hat{\mathbf{n}})$  the distribution function of photons in the plasma with momentum along the unit vector  $\hat{\mathbf{k}}$  at the last scattering surface in the sky direction  $\hat{\mathbf{n}}$ . This distribution function does not depend on the polarization of the photons because the incoming radiation is taken to be unpolarized. Using the expression of the Thomson cross section (6.67), the Stokes parameter  $Q(\hat{\mathbf{n}})$  can be written as

$$Q(\hat{\mathbf{n}}) \sim \sum_{a=1,2} \int d\Omega(\hat{\mathbf{k}}) f(\hat{\mathbf{k}}, \hat{\mathbf{n}}) \left[ |\varepsilon(\mathbf{k}, a) \cdot \hat{\mathbf{e}}_{\leftrightarrow}|^2 - |\varepsilon(\mathbf{k}, a) \cdot \hat{\mathbf{e}}_{\updownarrow}|^2 \right], \quad (6.71)$$

where we integrate over the directions of the incoming photons and have omitted a global normalization constant. To write this expression we have taken the intensity of scattered radiation to be proportional to the Thomson differential cross section averaged over polarizations. The result is integrated over the direction of the incoming photons weighted by the distribution function. The sum over polarizations can be explicitly done using the result derived in Eq. (6.69) to give

$$Q(\hat{\mathbf{n}}) \sim -\frac{1}{2} \int d\Omega(\hat{\mathbf{k}}) f(\hat{\mathbf{k}}, \hat{\mathbf{n}}) \left[ (\hat{\mathbf{k}} \cdot \hat{\mathbf{e}}_{\leftrightarrow})^2 - (\hat{\mathbf{k}} \cdot \hat{\mathbf{e}}_{\updownarrow})^2 \right]. \quad (6.72)$$

In order to evaluate the parameter  $U(\hat{\mathbf{n}})$  we need to consider the polarizations along the unit vectors defined by (see right panel in Fig. 6.4)

$$\hat{\mathbf{e}}_{\nearrow} = -\frac{1}{\sqrt{2}}(\hat{\mathbf{e}}_{\varphi} + \hat{\mathbf{e}}_{\theta}), \quad \hat{\mathbf{e}}_{\nwarrow} = -\frac{1}{\sqrt{2}}(\hat{\mathbf{e}}_{\varphi} - \hat{\mathbf{e}}_{\theta}). \quad (6.73)$$

This parameter is then given by the difference in intensity of the scattered radiation with these polarizations, namely

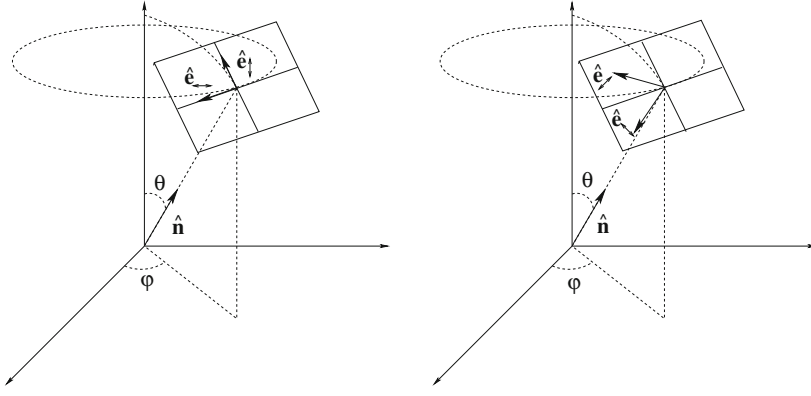


**Fig. 6.4** Polarization states used to define the Stokes parameter  $Q(\hat{\mathbf{n}})$  and  $U(\hat{\mathbf{n}})$  for a photon scattered by a nonrelativistic electron and arriving from the direction  $\hat{\mathbf{n}}$ . The notation used in the unit vectors  $\hat{\mathbf{e}}_{\nearrow}$  and  $\hat{\mathbf{e}}_{\searrow}$  reflects the point of view of an observer located at the origin looking in the direction defined by  $\hat{\mathbf{n}}$

$$\begin{aligned}
 U(\mathbf{n}) &\sim \sum_{a=1,2} \int d\Omega(\hat{\mathbf{k}}) f(\hat{\mathbf{k}}, \mathbf{n}) \left[ |\varepsilon(\mathbf{k}, a) \cdot \hat{\mathbf{e}}_{\nearrow}|^2 - |\varepsilon(\mathbf{k}, a) \cdot \hat{\mathbf{e}}_{\searrow}|^2 \right] \\
 &= -\frac{1}{2} \int d\Omega(\hat{\mathbf{k}}) f(\hat{\mathbf{k}}, \hat{\mathbf{n}}) \left[ (\hat{\mathbf{k}} \cdot \hat{\mathbf{e}}_{\nearrow})^2 - (\hat{\mathbf{k}} \cdot \hat{\mathbf{e}}_{\searrow})^2 \right], \quad (6.74)
 \end{aligned}$$

where in the second line we have carried out the sum over incoming polarizations. A look at Fig. 6.4 shows that  $Q(\hat{\mathbf{n}})$  and  $U(\hat{\mathbf{n}})$  can be transformed into one another, up to a sign, by a rotation of  $\frac{\pi}{4}$  along the line of sight  $\hat{\mathbf{n}}$ .

Finally, the Stokes parameter  $V(\hat{\mathbf{n}})$  measures the net circular polarization of the CMB photons arriving from the last scattering surface

$$\begin{aligned}
 V(\hat{\mathbf{n}}) &\sim \sum_{a=1,2} \int d\Omega(\hat{\mathbf{k}}) f(\hat{\mathbf{k}}, \mathbf{n}) \left[ |\varepsilon(\mathbf{k}, a) \cdot \hat{\mathbf{e}}_+|^2 - |\varepsilon(\mathbf{k}, a) \cdot \hat{\mathbf{e}}_-|^2 \right] \\
 &= \int d\Omega(\hat{\mathbf{k}}) f(\hat{\mathbf{k}}, \mathbf{n}) \left[ |\hat{\mathbf{k}} \cdot \hat{\mathbf{e}}_+|^2 - |\hat{\mathbf{k}} \cdot \hat{\mathbf{e}}_-|^2 \right] = 0, \quad (6.75)
 \end{aligned}$$

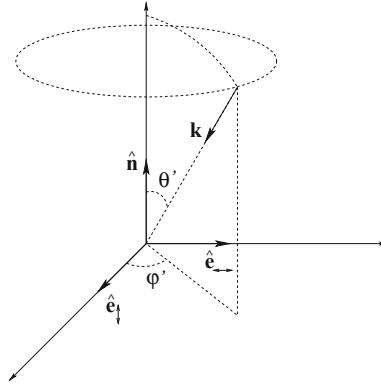
where  $\hat{\mathbf{e}}_{\pm} = -\frac{1}{\sqrt{2}}(\hat{\mathbf{e}}_{\varphi} \pm i\hat{\mathbf{e}}_{\theta})$  and the last identity follows immediately from  $\hat{\mathbf{e}}_{\pm}^* = \hat{\mathbf{e}}_{\mp}$ . This result reflects the fact that Thomson scattering does not distinguish between left and right polarizations.

The measurement of  $Q(\hat{\mathbf{n}})$  and  $U(\hat{\mathbf{n}})$  provides important information about the distribution function of photons at decoupling  $f(\hat{\mathbf{k}}, \hat{\mathbf{n}})$ , as we will see shortly. In order to carry out the integration over  $\hat{\mathbf{k}}$  in Eqs. (6.72) and (6.74) we use the system of coordinates defined by the three unit vectors  $\hat{\mathbf{e}}_{\uparrow}$ ,  $\hat{\mathbf{e}}_{\leftrightarrow}$  and  $\hat{\mathbf{n}}$ , as shown in Fig. 6.5. After a bit of algebra we arrive at

$$Q(\hat{\mathbf{n}}) \pm iU(\hat{\mathbf{n}}) \sim - \int d\Omega(\theta', \varphi') f(\theta', \varphi'; \hat{\mathbf{n}}) \sin^2 \theta' e^{\pm 2i\varphi'}, \quad (6.76)$$



**Fig. 6.5** A photon with momentum  $\mathbf{k}$  is scattered by a nonrelativistic electron located at the origin. The frame vectors  $\hat{\mathbf{n}}$ ,  $\hat{\mathbf{e}}_{\leftrightarrow}$  and  $\hat{\mathbf{e}}_{\updownarrow}$  are the ones shown in the left panel of Fig. 6.4



where the dependence on the unit vector  $\hat{\mathbf{k}}$  is indicated by its polar coordinates  $(\varphi', \theta')$ .

There is something very interesting about this expression. The functional dependence on  $\hat{\mathbf{k}}$  of the term multiplying  $f(\hat{\mathbf{k}}, \hat{\mathbf{n}})$  is that of the spherical harmonics

$$Y_2^{\pm 2}(\theta', \varphi') = 3\sqrt{\frac{5}{96\pi}} \sin^2 \theta' e^{\pm 2i\varphi'}. \quad (6.77)$$

Thus, the only way to make the integral (6.76) nonzero is that the distribution function  $f(\hat{\mathbf{k}}, \hat{\mathbf{n}})$  contains a quadrupole anisotropy. In other words, what we have concluded is that the measurement of the polarization of the CMB gives direct information about the quadrupole component of the distribution function of photons at decoupling!

The distinction between  $Q(\hat{\mathbf{n}})$  and  $U(\hat{\mathbf{n}})$  is rather arbitrary, since one parameter can be transformed into the other by an appropriate rotation along  $\hat{\mathbf{n}}$ . In fact, under such a rotation of angle  $\phi$  the complex combinations of the two Stokes parameters in Eq. (6.76) transform as

$$Q(\hat{\mathbf{n}}) \pm iU(\hat{\mathbf{n}}) \longrightarrow e^{\mp 2i\phi} [Q(\hat{\mathbf{n}}) \pm iU(\hat{\mathbf{n}})]. \quad (6.78)$$

Now,  $Q(\hat{\mathbf{n}}) \pm iU(\hat{\mathbf{n}})$  defines two complex functions on the two-dimensional sphere whose points are labelled by the unit vector  $\hat{\mathbf{n}}$ . Eq. (6.78) defines a local  $SO(2)$  rotations in the sphere under which  $Q(\hat{\mathbf{n}}) \pm iU(\hat{\mathbf{n}})$  transform as quantities with spin  $\pm 2$ . Were they scalars, we could expand them using the ordinary spherical harmonics  $Y_\ell^m(\hat{\mathbf{n}})$ . Due however to their nontrivial transformation properties, the expansion has to be made in terms of a basis of eigenfunctions of the Laplace operators on the sphere  $S^2$  with the appropriate transformations under  $SO(2)$  local rotations. The sought for basis of functions are generalizations of the standard spherical harmonics called the spin-weighted spherical harmonics of spin  $\pm 2$ , denoted by  ${}_{\pm 2}Y_\ell^m(\hat{\mathbf{n}})$ . Here we will not elaborate on their properties (see [2] for details). For us it is enough to know that they can be used to write the expansion